https://doi.org/10.5194/egusphere-2025-654
Preprint. Discussion started: 20 March 2025

Measurement report: Simultaneous measurement on atmospheric gas- and aerosol-phase water-soluble organics in Shanghai: Remarkable increase in light absorbing of Asian dust aerosols during long-range transport

Zheng Li[1], Gehui Wang[1,2]*, Binyu Xiao[1], Rongjie Li[1], Can Wu[1,2]*, Shaojun Lv[1], Feng Wu[3], Qingyan Fu[4], Yusen Duan[5]

[1]Key Lab of Geographic Information Science of the Ministry of Education, School of Geographic Sciences, East China Normal University, Shanghai 210062, China
[2]Institute of Eco-Chongming, 20 Cuiniao Rd., Chongming, Shanghai 202150, China
[3]State Key Laboratory of Loess and Quaternary Geology, Institute of Earth Environment, Chinese Academy of Science, Xi'an 710061, China
[4]Key Laboratory of Formation and Prevention of Urban Air Pollution Complex, Ministry of Ecology and Environment, Shanghai Academy of Environmental Sciences, Shanghai, 200233, China
[5]Shanghai Technology Center for Reduction of Pollution and Carbon Emissions, Shanghai, 200233, China

Correspondence to: Prof. Gehui Wang (ghwang@geo.ecnu.edu.cn) and Dr. Can Wu (cwu@geo.ecnu.edu.cn)

https://doi.org/10.5194/egusphere-2025-654
Preprint. Discussion started: 20 March 2025

Abstract: To better understand physicochemical evolution of Asian dust particles during long-range transport, water-soluble organic compounds (WSOCs) in gas- ($WSOC_g$) and particle-phase ($WSOC_p$) were simultaneously measured with a 1-hr time resolution in Shanghai during the 2023 dust storm (DS) and haze event (HE), and characterized for their optical properties and size distribution. Our results showed that gas-to-particle-phase partitioning coefficients (F_p) of WSOCs in DS (0.3 ± 0.06) was comparable to that in HE (0.32 ± 0.06), although both temperature and relative humidity in DS were not favorable for the partitioning, indicating a promoting role of dust particles in the transformation process of $WSOC_g$ from the gas to the particle phase. F_p variation was largely driven by aerosol liquid water content in HE but by aerosol acidity in DS. $WSOC_p$ and its light absorption at λ_{365nm} dominated at the fine mode (< 2.1 μm) in HE and the coarse mode (> 2.1 μm) in DS, respectively. Mass absorption coefficient (MAC) of the coarse mode of $WSOC_p$ at λ_{365nm} in DS was 0.8 $m^2\ g^{-1}$, which is four times that (0.20 ± 0.09 $m^2\ g^{-1}$) in the source region of Tengger Desert, suggesting a remarkably increase in light absorbing ability of Asian dust during long-range transport. Sharp co-increases of nitroaromatics, imidazoles, and water-soluble organic nitrogen at the coarse mode in the DS period further revealed that such an increasing MAC is mainly caused by adsorption and heterogeneous formation of light absorbing nitrogen-containing organics on the dust surface during long-range transport.

https://doi.org/10.5194/egusphere-2025-654
Preprint. Discussion started: 20 March 2025

1 Introduction

Dust storm (DS) release up to 2 billion tons of dust particles into the global atmosphere annually, exerting significant impacts on visibility, climate, and ecological environment (Li et al., 2014a; Tang et al., 2016; Wu et al., 2020; Chen et al., 2023; Ge et al., 2024). During a long range transport physicochemical properties of dust particles can significantly be changed by a series of chemical reactions especially in the downwind region of East Asia, where anthropogenic gas pollutants are abundant (Wang et al., 2014; Wang et al., 2015; Zhang et al., 2015; Wu et al., 2020).

Since the majority of oxidation products of atmospheric volatile organic compounds (VOCs) are water-soluble, gas-to-particle-phase partitioning of water-soluble organic compounds (WSOCs) is a major formation pathway of SOA in the atmosphere (Ervens et al., 2011; Liu et al., 2012; Gkatzelis et al., 2021; Lv et al., 2022b; Lv et al., 2022a). The gas-to-particle-phase partitioning process is regulated by a variety of factors such as concentrations of VOCs and NO_x and their compositions, in addition to temperature and relative humidity (RH) (Hennigan et al., 2009; El-Sayed et al., 2018). In the past decade, atmospheric environment in East Asia has changed significantly due to sharp reductions in SO_2 and black carbon (BC) emissions in China, which is currently dominated with NOx, VOCs and ammonia along with an increasing level of O_3 (Zhang et al., 2020; Liu et al., 2022; Xiao et al., 2022; Wang et al., 2023; Chen et al., 2024). Dust storm from East Asia desert regions is one of the major contributors to the global atmospheric aerosols (Li et al., 2014b; Wang et al., 2020). Such a change in the East Asia atmospheric environment could also significantly alter the physicochemical evolution process of dust particles during long range transport by adsorption and reactions such as gas-to-particles partitioning of WSOCs onto dust particle surface and SOA formation on the wetted dust. Therefore, field

https://doi.org/10.5194/egusphere-2025-654
Preprint. Discussion started: 20 March 2025

observations on the gas-to-particle-phase partitioning of WSOCs is necessary for better understanding on SOA formation process in the current East Asia atmosphere.

A few studies has indicated that gas-to-particle phase partitioning of WSOCs in China is much more efficient than that in developed countries such as the United States, mainly due to a high level of NH_3 in China (Zhang et al., 2012; Lv et al., 2022b; Lv et al., 2022a). Our recent observation found that such an enhanced gas-to-particle phase partitioning in China not only increase SOA production but also promote the atmospheric aerosol light absorption (Liu et al., 2023). Up to date, most of field investigations on WSOCs partitioning and organic aerosol light absorption have been conducted in winter with a focus on fine particle pollution (Cheng et al., 2016; Yuan et al., 2020; Lv et al., 2022b; Li et al., 2023a; Li et al., 2023b; Liu et al., 2024). In contrast, WSOC partitioning behavior and organic aerosol light absorption in East Asia during spring has rarely been investigated, where dust particles and NH_3 in the troposphere are much more abundant in spring than in winter. In this study we performed a simultaneous measurement on the atmospheric gas- and aerosol-phase WSOCs in Shanghai with a focus on the heterogenous formation of SOA on dust surface and its impact on dust particle optical properties. Our work for the first time unveiled that light absorbing ability of Asian dust is remarkably enhanced during long range transport by formation of light absorbing SOA, which is termed as brown carbon, on dust particle surface.

2 Materials and methods

2.1 Samples collection

The filed observation was conducted from 27 March to 21 April 2023 on the campus of East China Normal University (31.03°, 121.45°), which is situated on the southern area of Shanghai. All instruments were set on the roof of the Atmospheric Observation Station with

https://doi.org/10.5194/egusphere-2025-654
Preprint. Discussion started: 20 March 2025

the air inlet 10 meters above the ground. A modified in-situ gas and aerosol compositions monitor (IGAC, Model 63GA, Fortelice International Co., Ltd., Taiwan, China) was used to synchronously measure gaseous and particulate speciess with a 3 hr interval for WSOCs and a 1-hr interval for inorganic ions, respectively (Lv et al., 2022b; Lv et al., 2022a). The collection efficiency for both gas- and aerosol- phase species is >73% (see the details in the supporting information). $PM_{2.5}$ filter samples were collected on a day/night basis by using a high-volume sampler (1.13 m^3 min^{-1}, TISCH Environmental, Inc.). Moreover, size-segregated aerosols were also collected by using a 9-stage sampler at an airflow rate of 28.3 L min^{-1} with cutoff points of 0.43, 0.65, 1.1, 2.1, 3.3, 4.7, 5.8 and 9.0 μm,respectively. PM_{10} samples during a dust event of 2023 were also collected in Tengger Desert, which is one of the major dust source regions in East Asia. All of the filter samples were collected onto the pre-baked (450 °C) quartz filters and stored in a freezer (−18 °C) prior to analysis.

Hourly $PM_{2.5}$ and PM_{10} mass concentrations were obtained from the Shanghai Environmental Monitoring Center. The meteorological factors, including temperature and RH, was monitored by an automatic weather station (MILOS520, Vaisala, Inc., Finland).

2.2 Chemical analysis

Several punches (1.5 cm diameter) of each filter sample were ultrasonically extracted by 45 mL Milli-Q water; the extracts were subsequently filtered with 0.45 μm syringe filter, in which inorganic ions (Na^+, NH_4^+, K^+, Mg^{2+}, Ca^{2+}, Cl^-, NO_2^-, NO_3^-, SO_4^{2-}), organic acids (formic, acetic, oxalic acids, pyruvic acid (Pyr) and methanesulfonic acid (MSA)) and WSOC were quantified by an ion chromatography (ICS-5000+, Themo Scientific) and a total organic carbon and total nitrogen (TOC/TN) analyzer (TOC-L CPH, Shimadzu, Japan), respectively. Meanwhile, optical absorption of WSOC in $PM_{2.5}$ and all other filter samples was measured using a liquid waveguide capillary UV–Vis spectrometer coupled with a long

https://doi.org/10.5194/egusphere-2025-654
Preprint. Discussion started: 20 March 2025

effective path length (1 m). The online measurements on the above species were also conducted by the modified IGAC system (Lv et al., 2022b; Lv et al., 2022a).

Nitroaromatics (NACs)including nitrophenols in the filter samples were extracted by a mixture of methanol and dichloromethane (2:1, v:v), derivatized with N,O-bis-(trimethylsilyl)trifluoroacetamide (BSTFA) and quantified by a gas chromatography (GC, HP7890B) coupled with mass spectroscopy (MS, HP5977B) (Wang et al., 2009). In addition, a total of eight imidazole compounds (IMs) were determined by using a high-performance liquid chromatography (HPLC, Thermo Scientific) coupled with orbitrap-mass spectrometry. The detailed method for the organic aerosol analysis can be found elsewhere (Li et al., 2020; Li et al., 2023a; Liu et al., 2023).

2.3 Calculations on ALWC and pH of $PM_{2.5}$

ALWC and pH were estimated using the thermodynamic model ISORROPIA-II, based on the hourly measured NH_3, RH, T and $PM_{2.5}$-related chemical compounds. A forward metastable mode was chosen for the calculation (Wang et al., 2016; Wang et al., 2018; Liu et al., 2024). The samples collected under RH > 95% conditions were excluded in this study, because RH > 95% conditions could increase ALWC and pH estimation uncertainties.

3 Results and discussion

3.1 Chemical characteristics of different aerosol pollution events

During the campaign $PM_{2.5}$ varied from 3 to 87 μg m^{-3} with an average of 30 ± 14 μg m^{-3} (Figure 1 and Table 1), which is slightly lower than the National Air Quality I Grade Standard (35 μg m^{-3}). However, particle pollution with a daily $PM_{2.5}$ > 35 μg m^{-3} were frequently observed during the campaign (Figure 1). In this study, a pollution event lasting for more than two consecutive days with a daily $PM_{2.5}$ levels > 35 μg m^{-3} was defined as a haze episode. As shown in Figure 1b, a dust storm event had occurred in Shanghai from 11

https://doi.org/10.5194/egusphere-2025-654
Preprint. Discussion started: 20 March 2025

to 13 April with a PM_{10} concentration sharply increasing to 986 μg m^{-3}, resulting in the $PM_{2.5}/PM_{10}$ mass ratio down to less than 0.1 and Ca^{2+} up to 2.5 μg m^{-3} (Table 1 and Figure 1). Thus, here we classified the observation periods of 5-9, 11-13, April as a haze event (HE) and dust storm event (DS), respectively. While those periods with a daily $PM_{2.5}$ < 35 μg m^{-3} was defined as a clean period (CP), which occurred from 18-22, April (Figure 1).

As seen in Table 1, secondary ions (sulfate, nitrate, ammonium, SNA) were the dominant species among the detected components. The mass contribution of SNA to $PM_{2.5}$ reached up to ~69 % in HE, which was 1.6-fold of that in CP, indicating a key role of SNA in the haze formation process. During the DS period, SNA loadings in Shanghai were comparable to that in CP, which only accounted for ~17 % of $PM_{2.5}$. However, the proportion is still remarkably higher than those in desert source and upwind regions (Table S1), indicating a significant formation of SNA during the dust long-transport. Ca^{2+}, Na^{+} and Mg^{2+} were 4–8 times higher in DS than in HE. Such enhancements in metal cations affected the aerosol acidity, resulting in the fine particles ($PM_{2.5}$) pH rising from 3.3 in non-dust storm period (NDS) to 7.5 in DS (Figure 1b).

As shown in Table 1, there was a large variability in $WSOC_g$ concentration, which ranged from 0.7 to 19.6 μgC m^{-3} with an average loading of 8.2 ± 3.3 μgC m^{-3} in the CP period and was higher than those in the HE and DS periods (Table 1). The partitioning coefficient of WSOC ($F_p = WSOC_p / (WSOC_p + WSOC_g)$) (0.32 ± 0.06, Table1) in HE was 33% higher than that in CP (0.24 ± 0.06, Table1) and robustly correlated with $WSOC_p$ (r = 0.68, p < 0.01) (Figure S1a). A similar strong correlation of $PM_{2.5}$ with $WSOC_p$ was also observed in HE but not in DS (Figure S1b). Since most components of SOA are water-soluble, such a strong correlation between F_p and $WSOC_p$ suggests that gas-to-particle-phase partitioning of WSOC is a major formation pathway of SOA in the HE period. WSOC level

https://doi.org/10.5194/egusphere-2025-654
Preprint. Discussion started: 20 March 2025

and F_p in DS (0.3 ± 0.06, Table1) was similar to those in HE and exhibited a well correlation each other (r = 0.61, p < 0.01) (Figure S1a), indicating that gas-to-particle partitioning of $WSOC_g$ was also an important formation pathway for SOA in the DS period.

3.2 Factors driving WSOC partitioning during aerosol pollution events

As shown in Table 1 and Figure 2a, ALWC in HE was 2.5-fold higher than that in CP period and well correlated with F_p (r = 0.66, p < 0.01), because $PM_{2.5}$ aerosols in the HE period were enriched in hygroscopic SNA, resulting in a high level of ALWC under the humid conditions (Table 1). Thus, ALWC took a key factor controlling the partitioning process of WSOC, similar to the results observed during winter in Shanghai, China and Los Angeles and Atlanta, United States (Hennigan et al., 2009; Zhang et al., 2012; Lv et al., 2022b). In contrast, ALWC in the DS period was much lower than that in the HE period with no correlation with F_p (Figure 2a), because SNA concentrations were much less in the DS period than those in the HE period. Moreover, RH in the DS period was 44 ± 18%, which is lower than the deliquescent point of SNA (Wang et al., 2016). Therefore, WSOC partitioning process during the DS was not regulated by ALWC. In this study, we calculated the contributions of organic matter (OM) and water-soluble inorganic ions to ALWC in the HE period. It can be seen from Figure S2a, NH_4NO_3 was the largest contributor to ALWC during the haze pollution period, followed by $(NH_4)_2SO_4$ and OM, with the contributions being 56.4 ± 12.2 %, 29.1 ± 7.1 %, and 6.1 ± 3.8 %, respectively. Figure 2b shows that ALWC increased exponentially along with the NH_3-partitioning coefficient ($\varepsilon(NH_4^+) = NH_4^+ / (NH_3 + NH_4^+)$) in the HE period and $WSOC_p$ increased in tandem with increases in ALWC in HE, which increased along with TNH_x concentrations (Figure 2c). Moreover, as seen in Figure 2d, $WSOC_p$ well correlated with TNH_x (= $NH_3 + NH_4^+$) in HE (r =0.72, p < 0.01), indicating that abundant ammonia in the atmosphere of Shanghai is favorable for WSOC partitioning

https://doi.org/10.5194/egusphere-2025-654
Preprint. Discussion started: 20 March 2025

and SOA formation. Na et al (2007) and Liu et al (2021) reported that NH_3 can be neutralized with organic acids to form ammonium salts, thus induce rapid increase in SOA yields. It can be seen from Figure S2b that particulate carboxylates exponentially increased along with an increase of TNH_x concentration, further demonstrating that NH_3 neutralization with organic acids was also responsible for the strong correlations of TNH_x with F_p in the HE period.

During the DS period, F_p of WSOCs robustly correlated with pH ($r = 0.98$, $p < 0.01$, Figure 2e), suggesting that pH was a key factor controlling the WSOC partitioning. As we discussion before, ammonia play an important role in $WSOC_p$ formation during the HE period with a strong correlation with TNH_x in HE (Figure 2d). However, such a correlation was not observed in DS (Figure 2d), which indicates that ammonia was not an effective factor driving the WSOC partitioning process in the DS period. As shown in Figure 2f, the sum of Ca^{2+}, Na^+ and Mg^{2+} concentrations showed a significantly correlation with particulate organic acids ($r = 0.88$, $p < 0.01$), including formic, acetic and oxalic acids, during the DS period, because the lower acidity of aerosols in the DS period was favorable for the reactive uptake of acidic organics by dust surface (Table 1).

3.3 Gas-to-particle partitioning of WSOC on size-resolved particles

Figure 3 shows the size distributions of water-soluble organic species, including $WSOC_p$, NACs, IMs and $WSON_p$, in the non-dust storm (NDS) and dust storm (DS) periods in Shanghai during the campaign. As shown in Figure 3a, $WSOC_p$ showed a bimodal size distribution pattern in both periods. The relative abundance of $WSOC_p$ in the coarse mode (> 2.1 μm) accounted for 59 % of the total during the DS period, which is 25 % higher than that in the NDS period. Oxalic, pyruvic and methanesulfonic acids are typical SOA tracers in the atmosphere (Wang et al., 2012; Huang et al., 2014; Wang et al., 2015; Wang et al., 2016;

https://doi.org/10.5194/egusphere-2025-654
Preprint. Discussion started: 20 March 2025

Tang et al., 2019), which displayed a bimodal pattern in the NDS period with two peaks distributing in the fine and coarse modes, respectively (Figure S3). In contrast, those secondary SOA presented a monomodal size distribution pattern in the DS period with a predominant peak in the coarse mode only. As seen in Table 2, their concentrations are substantially higher than those in the Tengger Desert region and mostly stayed in the coarse mode (> 2.1μm) during the DS period (Table 2), clearly revaling an enhanced SOA formation on the dust particles during their transport from the Asian desert source region to the downwind city. As shown in Figure S4, F_p of WSOC in the fine and coarse modes were larger than those in the NDS period, especially for the coarse mode of Fp, which was 60 % higher in the DS period than that in the NDS period, indicating that dust surface is favorable for the uptake of $WSOC_g$.

Previous studies reported that NACs can be formed secondarily via both gas-phase and aqueous-phase reaction pathways (Wang et al., 2019; Hems et al., 2020; Ren et al., 2023). For example, benzene reacts with OH radicals and generates phenol. Then, phenol further reacts with NO_2 and yields gaseous nitrophenol (Liang et al., 2020). The latter subsequently partitions to the condensed phase (Lauraguais et al., 2014). Moreover, phenol and catechol can also react with NO_2 radical in the aerosol aqueous phase to form the corresponding NACs (Vione et al., 2004). Our recent study in Shanghai found that the gaseous NACs (i.e., nitrophenol and methylnitrophenols) concentrations were 2 orders of magnitude higher than the particulate ones (Liu et al., 2023). As seen in Figure 3b, NACs showed a bimodal pattern with a relatively larger peak in the coarse mode during the NDS period. In contrast, NACs almost entirely stayed in the coarse mode during the DS event. Such distinct size distribution patterns indicate that NACs in Shanghai in the DS event were mainly formed by a gas-phase oxidation and subsequent partitioning onto the dust surface.

https://doi.org/10.5194/egusphere-2025-654
Preprint. Discussion started: 20 March 2025

IMs can be directly emitted from biomass burning process and secondarily produced from reactions of carbonyls with amines and ammonia in aerosol aqueous phase (Lian et al., 2021; Liu et al., 2023). As shown in Figure 3c, IMs predominantly stayed in the fine mode in the NDS period. However, in the DS period IMs showed a bimodal pattern in the DS period with two equivalent peaks in the fine and coarse modes. respectively. Since IMs were not detected in the Desert source samples (Table 2), the peak of IMs in the coarse particles in Shanghai during the DS period are expected to be secondarily formed on the dust particles via heterogeneous reactions such as the reactions of glyoxal and methylgloxoal with free NH_3 molecules in aerosol aqueous phase (Liu et al., 2023). Size-resolved chemistry analysis results showed that NO_3^- in the coarse mode poorly correlated with NH_4^+ (> 2.1 μm) in the NDS period ($r = 0.29$, $p < 0.05$) but robustly correlated with NH_4^+ ($r = 0.76$, $p < 0.01$) in the DS period (Figure S5a). Field observations found that NO_3^- in the coarse mode during the NDS period is formed via reaction uptake of gaseous HNO_3 by coarse particles and exists mostly as $Ca(NO_3)_2$. Therefore, NO_3^- in coarse particles poorly correlates with NH_4^+ (Figure S5a), because coarse particles are usually enriched with $CaCO_3$, which is more basic than NH_3. However, in a typical Asian dust storm period the coarse mode of NO_3^- usually strongly correlates with NH_4^+, because there are large amounts of mineral dust particles in Asian dessert region such as Na_2SO_4, $CaSO_4$ and NaCl (Wu et al., 2020). Those mineral dust particles are hygroscopic and can promote the hydrolysis of N_2O_5 on dust particle surface and produce HNO_3, which subsequently neutralize with NH_3 as NH_4NO_3 (Wang et al., 2014; Wu et al., 2020). Therefore, a linear correlation between NO_3^- and NH_4^+ in the coarse mode was observed in Shanghai in DS during the campaign (Figure S5a). As we discussed in section 3.2, NH_4NO_3 was the biggest contributor to ALWC in the NDS periods (Xie et al., 2020; Lv et al., 2022b). Therefore, the formation of hygroscopic species such as NH_4NO_3

https://doi.org/10.5194/egusphere-2025-654
Preprint. Discussion started: 20 March 2025

can enhance gas-to-particle phase partitioning of $WSOC_g$ and the heterogeneous reactions on the dust surface. Similarly, the coarse mode of oxalic acid robustly and linearly correlated with NH_4^+ in the DS period but not correlated with NH_4^+ in the NDS period ($r = 0.97$, $p < 0.01$) (Figure S5b), which again suggests an enhanced heterogeneous reaction of SOA on the mineral particle surface during Asian dust long-range transport.

3.4 Enhanced light absorption ability of Asian dust particles

As seen in Figure 3d, $WSON_p$ presented a monomodal size distribution pattern in Shanghai, peaking at the fine and coarse mode in the NDS and DS periods, respectively. The relative abundance of $WSON_p$ in the coarse mode in the DS period is 0.8 times higher than that in the NDS period. Such an increased $WSON_p$ in the coarse mode in the DS period is in good agreement with that of NACs and IMs and indicates an enhanced formation of nitrogen-containing organic compounds on dust surface (Figure 3b-d).

Previous researches have shown that many of nitrogen-containing organic compounds in the troposphere are light absorbing brown carbon (BrC) (Laskin et al., 2015; Liu et al., 2024; Laskin et al., 2025). Thus, here we further investigate the optical properties of the dust samples. As seen in Table 2, Abs_{365} (1.9 M m^{-1}) and MAC_{365} (1.0 m^2 g^{-1}) of BrC in the fine mode during the NDS period were comparable to those during the DS period (2.2 M $m^{-1}$and 0.9 m^2 g^{-1}, respectively). However, Abs_{365} and MAC_{365} (2.6 M m^{-1}, 0.8 m^2 g^{-1}, Table 2) in the coarse mode in the DS period were 2–3 times higher those (0.8 M m^{-1}, 0.4 m^2 g^{-1}, Table 2) in the NDS period, respectively, suggesting an enhanced light absorption of coarse particle in the Asian dust storm events. To reveal the nature of such an increase in light absorption of dust particles, we measured the optical properties of atmospheric PM_{10} collected in Tengger Desert. As shown in Figure 4a, MAC of water-soluble BrC in total suspended particles (TSP) in the wavelength range of $\lambda = 250–500$ nm in Shanghai during

https://doi.org/10.5194/egusphere-2025-654
Preprint. Discussion started: 20 March 2025

the DS period is slightly higher than that in the NDS period, but is more than two times that in Tengger Desert region, suggesting a remarkable increase in light absorption ability of TSP in the downwind city during both NDS and DS periods. MAC_{365} of BrC in the coarse mode during the DS period in Shanghai (0.8 m^2 g^{-1}, Table 2) is four times that in Tengger Desert regions (0.2 ± 0.09 m^2 g^{-1}, Table 2). As shown in Figure 4b, $MAC_{250\text{-}600}$ of water-soluble BrC in the fine mode during both sampling periods were comparable, but the $MAC_{250\text{-}600}$ in the coarse mode during DS period was significantly higher than that in NDS period. Such an increase in light absorption that only occurred in the coarse mode clearly demonstrates that light absorption ability of Asian dust particles in the DS period was significantly strengthened during the long-range transport, which is mostly due to an efficient formation of nitrogen-containing organic compounds on the dust surface.

4 Summary and implications

In this study we synchronously measured the hourly concentrations of gaseous and particulate WSOC in Shanghai, a downwind city of East Asian desert sources, along with measurements on organic tracers and inorganic ions in the gas- and aerosol- phases. We found that the gas-to-aerosol-phase partitioning coefficient (Fp) of WSOC on the dust storm days (0.3 ± 0.06) in the city is comparable to that on the haze days (0.32 ± 0.06), although the meteorological conditions were drier and hotter during the dust storm period and thus not favorable for the WSOC partitioning, suggesting an enhancing effect of dust particles on the SOA formation on the dust particle surface. In this study, we found the F_p variation was influenced by ALWC in HE but by pH in DS. Moreover, $WSOC_p$ and its light absorption at λ_{365nm} in the coarse mode was increased significantly in DS period than in NDS period. Notably, by comparing with the aerosol optical properties in Tengger desert, we further found that Asian dust aerosols became much more light absorbing with a MAC_{365} four times

https://doi.org/10.5194/egusphere-2025-654
Preprint. Discussion started: 20 March 2025

that in the Asian dust source region, which is caused by the enhanced SOA formation on the dust surface during the long-range transport through adsorption and heterogenous formation of light-absorbing brown carbon including nitrogen-containing organics such as nitroaromatics and imidazoles.

Atmospheric nitroaromatics and imidazoles are mostly produced from the reactions of aromatic with NO_x in the gas phase and carbonyls with free NH_3 in the aerosol aqueous phase, respectively (Liu et al., 2023; Liu et al., 2024). Although atmospheric SO_2 level in China has been decreased significantly due to strict emission control, the concentrations of NO_x, VOCs and NH_3 in the country are still very high, resulting in SOA in the country much more light absorbing than those in USA and other developed countries. Our previous studies found that secondary brown carbon is much more favorably formed under a high pH conditions (Liu et al., 2023; Zhang et al., 2024), because (1) nitrophenols are acidic species and thus easier to be adsorbed onto dust surface, and (2) a high pH condition favors NH_4^+ dissociate into $NH_3 + H^+$ and thus can promote the reaction of carbonyl with NH_3.

Currently, global aerosol model ensemble estimate that the global dust direct radiative effects is about -0.4 W m^2 (Kok et al., 2017). However, by using an analysis on the size and abundance of dust aerosols to constrain the global model, Abedibi and Kok (2020) found that dust aerosols in the atmosphere is coarser than the size estimated by the current global model ensemble and the dust direct radiative effect is +0.15 W m^2, which means that dust cause a net warming of the planet. Based the results given by this study, we think that global direct radiative effect of dust aerosol is possibly more warming if the secondary formation of light absorbing brown carbon is accounted for.

Data Availability.

https://doi.org/10.5194/egusphere-2025-654
Preprint. Discussion started: 20 March 2025

The data including meteorological data, gaseous pollutants, and major chemical components in $PM_{2.5}$ are freely available at https://doi.org/10.5281/zenodo.14883402 (Li, 2025).

Author Contributions

GW designed the experiment and supervised the research. ZL, BX, RL and FW collected the samples. ZL, CW, BX, and GW conducted the sample analysis. ZL, BX, CW, RL, and GW performed the data interpretation. ZL, CW and GW wrote the paper. All the authors contributed to the paper with useful scientific discussions.

Notes

The authors declare no competing financial interest.

Acknowledgement:

This work was funded by the National Natural Science Foundation of China (No. 42130704, U23A2030), and the National Key Research and Development Program of China (2023YFC3706302).

https://doi.org/10.5194/egusphere-2025-654
Preprint. Discussion started: 20 March 2025

References:

Adebiyi, A. A. and Kok, J. F.: Climate models miss most of the coarse dust in the atmosphere, Science Advances, 6, 10.1126/sciadv.aaz9507, 2020.

Chen, Q., Miao, R. Q., Geng, G. N., Shrivastava, M., Dao, X., Xu, B. Y., Sun, J. Q., Zhang, X., Liu, M. Y., Tang, G. G., Tang, Q., Hu, H. W., Huang, R. J., Wang, H., Zheng, Y., Qin, Y., Guo, S., Hu, M., and Zhu, T.: Widespread 2013-2020 decreases and reduction challenges of organic aerosol in China, Nature Communications, 15, 10.1038/s41467-024-48902-0, 2024.

Chen, S., Zhao, D., Huang, J., He, J., Chen, Y., Chen, J., Bi, H., Lou, G., Du, S., Zhang, Y., and Yang, F.: Mongolia Contributed More than 42% of the Dust Concentrations in Northern China in March and April 2023, Advances in Atmospheric Sciences, 40, 1549-1557, 10.1007/s00376-023-3062-1, 2023.

Cheng, Y., He, K. B., Du, Z. Y., Engling, G., Liu, J. M., Ma, Y. L., Zheng, M., and Weber, R. J.: The characteristics of brown carbon aerosol during winter in Beijing, Atmos Environ, 127, 355-364, 10.1016/j.atmosenv.2015.12.035, 2016.

El-Sayed, M. M. H., Ortiz-Montalvo, D. L., and Hennigan, C. J.: The effects of isoprene and NOx on secondary organic aerosols formed through reversible and irreversible uptake to aerosol water, Atmos Chem Phys, 18, 1171-1184, 10.5194/acp-18-1171-2018, 2018.

Ervens, B., Turpin, B. J., and Weber, R. J.: Secondary organic aerosol formation in cloud droplets and aqueous particles (aqSOA): a review of laboratory, field and model studies, Atmos. Chem. Phys., 11, 11069-11102, 10.5194/acp-11-11069-2011, 2011.

Ge, J., Li, W., Huang, J., Mu, Q., Li, Q., Zhao, Q., Su, J., Xie, Y., Alam, K., Zhu, Z., and Hu, X.: Dust Accelerates the Life Cycle of High Clouds Unveiled Through Strongly-Constrained Meteorology, Geophysical Research Letters, 51, e2024GL109998, https://doi.org/10.1029/2024GL109998, 2024.

Gkatzelis, G. I., Papanastasiou, D. K., Karydis, V. A., Hohaus, T., Liu, Y., Schmitt, S. H., Schlag, P., Fuchs, H., Novelli, A., Chen, Q., Cheng, X., Broch, S., Dong, H., Holland, F., Li, X., Liu, Y., Ma, X., Reimer, D., Rohrer, F., Shao, M., Tan, Z., Taraborrelli, D., Tillmann, R., Wang, H., Wang, Y., Wu, Y., Wu, Z., Zeng, L., Zheng, J., Hu, M., Lu, K., Hofzumahaus, A., Zhang, Y., Wahner, A., and Kiendler-Scharr, A.: Uptake of Water-soluble Gas-phase Oxidation Products Drives Organic Particulate Pollution in Beijing, Geophysical Research Letters, 48, e2020GL091351, https://doi.org/10.1029/2020GL091351, 2021.

Hems, R. F., Schnitzler, E. G., Bastawrous, M., Soong, R., Simpson, A. J., and Abbatt, J. P. D.: Aqueous Photoreactions of Wood Smoke Brown Carbon, ACS Earth and Space Chemistry, 4, 1149-1160, 10.1021/acsearthspacechem.0c00117, 2020.

Hennigan, C. J., Bergin, M. H., Russell, A. G., Nenes, A., and Weber, R. J.: Gas/particle partitioning of water-soluble organic aerosol in Atlanta, Atmos Chem Phys, 9, 3613-3628, DOI 10.5194/acp-

https://doi.org/10.5194/egusphere-2025-654
Preprint. Discussion started: 20 March 2025

9-3613-2009, 2009.

Huang, R.-J., Zhang, Y., Bozzetti, C., Ho, K.-F., Cao, J.-J., Han, Y., Daellenbach, K. R., Slowik, J. G., Platt, S. M., Canonaco, F., Zotter, P., Wolf, R., Pieber, S. M., Bruns, E. A., Crippa, M., Ciarelli, G., Piazzalunga, A., Schwikowski, M., Abbaszade, G., Schnelle-Kreis, J., Zimmermann, R., An, Z., Szidat, S., Baltensperger, U., Haddad, I. E., and Prévôt, A. S. H.: High secondary aerosol contribution to particulate pollution during haze events in China, Nature, 514, 218-222, 10.1038/nature13774, 2014.

Kok, J. F., Ridley, D. A., Zhou, Q., Miller, R. L., Zhao, C., Heald, C. L., Ward, D. S., Albani, S., and Haustein, K.: Smaller desert dust cooling effect estimated from analysis of dust size and abundance, Nature Geoscience, 10, 274-278, 10.1038/Ngeo2912, 2017.

Laskin, A., Laskin, J., and Nizkorodov, S. A.: Chemistry of Atmospheric Brown Carbon, Chemical Reviews, 115, 4335-4382, 10.1021/cr5006167, 2015.

Laskin, A., West, C. P., and Hettiyadura, A. P. S.: Molecular insights into the composition, sources, and aging of atmospheric brown carbon, Chem Soc Rev, 10.1039/d3cs00609c, 2025.

Lauraguais, A., Coeur-Tourneur, C., Cassez, A., Deboudt, K., Fourmentin, M., and Choël, M.: Atmospheric reactivity of hydroxyl radicals with guaiacol (2-methoxyphenol), a biomass burning emitted compound: Secondary organic aerosol formation and gas-phase oxidation products, Atmos Environ, 86, 155-163, https://doi.org/10.1016/j.atmosenv.2013.11.074, 2014.

Li, D. P., Wu, C., Zhang, S., Lei, Y. L., Lv, S. J., Du, W., Liu, S. J., Zhang, F., Liu, X. D., Liu, L., Meng, J. J., Wang, Y. S., Gao, J., and Wang, G. H.: Significant coal combustion contribution to water-soluble brown carbon during winter in Xingtai, China: Optical properties and sources, Journal of Environmental Sciences, 124, 892-900, 10.1016/j.jes.2022.02.026, 2023a.

Li, H., Qin, X., Chen, J., Wang, G., Liu, C., Lu, D., Zheng, H., Song, X., Gao, Q., Xu, J., Zhu, Y., Liu, J., Wang, X., Deng, C., and Huang, K.: Continuous Measurement and Molecular Compositions of Atmospheric Water-Soluble Brown Carbon in the Nearshore Marine Boundary Layer of Northern China: Secondary Formation and Influencing Factors, Journal of Geophysical Research: Atmospheres, 128, e2023JD038565, https://doi.org/10.1029/2023JD038565, 2023b.

Li, J. J., Li, J., Wang, G. H., Zhang, T., Dai, W. T., Ho, K. F., Wang, Q. Y., Shao, Y., Wu, C., and Li, L.: Molecular characteristics of organic compositions in fresh and aged biomass burning aerosols, Sci Total Environ, 741, 10.1016/j.scitotenv.2020.140247, 2020.

Li, W., Shao, L., Shi, Z., Chen, J., Yang, L., Yuan, Q., Yan, C., Zhang, X., Wang, Y., Sun, J., Zhang, Y., Shen, X., Wang, Z., and Wang, W.: Mixing state and hygroscopicity of dust and haze particles before leaving Asian continent, Journal of Geophysical Research: Atmospheres, 119, 1044-1059, https://doi.org/10.1002/2013JD021003, 2014a.

Li, W. J., Shao, L. Y., Shi, Z. B., Chen, J. M., Yang, L. X., Yuan, Q., Yan, C., Zhang, X. Y., Wang, Y. Q., Sun, J. Y., Zhang, Y. M., Shen, X. J., Wang, Z. F., and Wang, W. X.: Mixing state and

https://doi.org/10.5194/egusphere-2025-654
Preprint. Discussion started: 20 March 2025

hygroscopicity of dust and haze particles before leaving Asian continent, J Geophys Res-Atmos, 119, 1044-1059, 10.1002/2013jd021003, 2014b.

Li, Z.: Simultaneous measurement on atmospheric gas- and aerosol-phase water-soluble organics during dust storm period: a case study in Shanghai, Zenodo [data set], https://doi.org/10.5281/zenodo.14883402, 2025.

Lian, X., Zhang, G., Yang, Y., Lin, Q., Fu, Y., Jiang, F., Peng, L., Hu, X., Chen, D., Wang, X., Peng, P. a., Sheng, G., and Bi, X.: Evidence for the Formation of Imidazole from Carbonyls and Reduced Nitrogen Species at the Individual Particle Level in the Ambient Atmosphere, Environ Sci Tech Let, 8, 9-15, 10.1021/acs.estlett.0c00722, 2021.

Liang, Y. H., Wang, X. F., Dong, S. W., Liu, Z. Y., Mu, J. S., Lu, C. Y., Zhang, J., Li, M., Xue, L. K., and Wang, W. X.: Size distributions of nitrated phenols in winter at a coastal site in north China and the impacts from primary sources and secondary formation, Chemosphere, 250, 10.1016/j.chemosphere.2020.126256, 2020.

Liu, J., Zhang, X., Parker, E. T., Veres, P. R., Roberts, J. M., de Gouw, J. A., Hayes, P. L., Jimenez, J. L., Murphy, J. G., Ellis, R. A., Huey, L. G., and Weber, R. J.: On the gas-particle partitioning of soluble organic aerosol in two urban atmospheres with contrasting emissions: 2. Gas and particle phase formic acid, Journal of Geophysical Research: Atmospheres, 117, https://doi.org/10.1029/2012JD017912, 2012.

Liu, S., Huang, D., Wang, Y., Zhang, S., Liu, X., Wu, C., Du, W., and Wang, G.: Synergetic effects of NH3 and NOx on the production and optical absorption of secondary organic aerosol formation from toluene photooxidation, Atmos. Chem. Phys., 21, 17759-17773, 10.5194/acp-21-17759-2021, 2021.

Liu, X., Wang, H., Wang, F., Lv, S., Wu, C., Zhao, Y., Zhang, S., Liu, S., Xu, X., Lei, Y., and Wang, G.: Secondary Formation of Atmospheric Brown Carbon in China Haze: Implication for an Enhancing Role of Ammonia, Environ Sci Technol, 57, 11163-11172, 10.1021/acs.est.3c03948, 2023.

Liu, X., Wu, C., Li, Z., Li, R., Wang, F., Lv, S., Li, R., Zhang, F., Wang, H., Liang, C., Zhang, L., and Wang, G.: Atmospheric brown carbon in China haze is dominated by secondary formation, Sci Total Environ, 945, 173901, https://doi.org/10.1016/j.scitotenv.2024.173901, 2024.

Liu, Y. C., Zhan, J. L., Zheng, F. X., Song, B. Y., Zhang, Y. S., Ma, W., Hua, C. J., Xie, J. L., Bao, X. L., Yan, C., Bianchi, F., Petäjä, T., Ding, A. J., Song, Y., He, H., and Kulmala, M.: Dust emission reduction enhanced gas-to-particle conversion of ammonia in the North China Plain, Nature Communications, 13, 10.1038/s41467-022-34733-4, 2022.

Lv, S. J., Wu, C., Wang, F. L., Liu, X. D., Zhang, S., Chen, Y. B., Zhang, F., Yang, Y., Wang, H. L., Huang, C., Fu, Q. Y., Duan, Y. S., and Wang, G. H.: Nitrate-Enhanced Gas-to-Particle-Phase Partitioning of Water- Soluble Organic Compounds in Chinese Urban Atmosphere: Implications

https://doi.org/10.5194/egusphere-2025-654
Preprint. Discussion started: 20 March 2025

for Secondary Organic Aerosol Formation, Environ Sci Tech Let, 10.1021/acs.estlett.2c00894, 2022a.

Lv, S. J., Wang, F. L., Wu, C., Chen, Y. B., Liu, S. J., Zhang, S., Li, D. P., Du, W., Zhang, F., Wang, H. L., Huang, C., Fu, Q. Y., Duan, Y. S., and Wang, G. H.: Gas-to-Aerosol Phase Partitioning of Atmospheric Water-Soluble Organic Compounds at a Rural Site in China: An Enhancing Effect of NH3 on SOA Formation, Environ Sci Technol, 56, 3915-3924, 10.1021/acs.est.1c06855, 2022b.

Na, K., Song, C., Switzer, C., and Cocker, D. R.: Effect of Ammonia on Secondary Organic Aerosol Formation from α-Pinene Ozonolysis in Dry and Humid Conditions, Environ Sci Technol, 41, 6096-6102, 10.1021/es061956y, 2007.

Ren, Y., Wang, G., Wei, J., Tao, J., Zhang, Z., and Li, H.: Contributions of primary emissions and secondary formation to nitrated aromatic compounds in themountain background region of Southeast China, Atmos. Chem. Phys., 23, 6835-6848, 10.5194/acp-23-6835-2023, 2023.

Tang, M., Cziczo, D. J., and Grassian, V. H.: Interactions of Water with Mineral Dust Aerosol: Water Adsorption, Hygroscopicity, Cloud Condensation, and Ice Nucleation, Chemical Reviews, 116, 4205-4259, 10.1021/acs.chemrev.5b00529, 2016.

Tang, M., Guo, L., Bai, Y., Huang, R.-J., Wu, Z., Wang, Z., Zhang, G., Ding, X., Hu, M., and Wang, X.: Impacts of methanesulfonate on the cloud condensation nucleation activity of sea salt aerosol, Atmos Environ, 201, 13-17, https://doi.org/10.1016/j.atmosenv.2018.12.034, 2019.

Vione, D., Maurino, V., Minero, C., Lucchiari, M., and Pelizzetti, E.: Nitration and hydroxylation of benzene in the presence of nitrite/nitrous acid in aqueous solution, Chemosphere, 56, 1049-1059, https://doi.org/10.1016/j.chemosphere.2004.05.027, 2004.

Wang, G., Zhang, R., Gomez, M. E., Yang, L., Levy Zamora, M., Hu, M., Lin, Y., Peng, J., Guo, S., Meng, J., Li, J., Cheng, C., Hu, T., Ren, Y., Wang, Y., Gao, J., Cao, J., An, Z., Zhou, W., Li, G., Wang, J., Tian, P., Marrero-Ortiz, W., Secrest, J., Du, Z., Zheng, J., Shang, D., Zeng, L., Shao, M., Wang, W., Huang, Y., Wang, Y., Zhu, Y., Li, Y., Hu, J., Pan, B., Cai, L., Cheng, Y., Ji, Y., Zhang, F., Rosenfeld, D., Liss, P. S., Duce, R. A., Kolb, C. E., and Molina, M. J.: Persistent sulfate formation from London Fog to Chinese haze, Proceedings of the National Academy of Sciences, 113, 13630, 10.1073/pnas.1616540113, 2016.

Wang, G. H., Kawamura, K., and Lee, M.: Comparison of organic compositions in dust storm and normal aerosol samples collected at Gosan, Jeju Island, during spring 2005, Atmos Environ, 43, 219-227, 10.1016/j.atmosenv.2008.09.046, 2009.

Wang, G. H., Cheng, C. L., Meng, J. J., Huang, Y., Li, J. J., and Ren, Y. Q.: Field observation on secondary organic aerosols during Asian dust storm periods: Formation mechanism of oxalic acid and related compounds on dust surface, Atmos Environ, 113, 169-176, 10.1016/j.atmosenv.2015.05.013, 2015.

https://doi.org/10.5194/egusphere-2025-654
Preprint. Discussion started: 20 March 2025

491 Wang, G. H., Kawamura, K., Cheng, C. L., Li, J. J., Cao, J. J., Zhang, R. J., Zhang, T., Liu, S. X.,
492 and Zhao, Z. Z.: Molecular Distribution and Stable Carbon Isotopic Composition of Dicarboxylic
493 Acids, Ketocarboxylic Acids, and α-Dicarbonyls in Size-Resolved Atmospheric Particles From
494 Xi'an City, China, Environ Sci Technol, 46, 4783-4791, 10.1021/es204322c, 2012.
495 Wang, G. H., Cheng, C. L., Huang, Y., Tao, J., Ren, Y. Q., Wu, F., Meng, J. J., Li, J. J., Cheng, Y. T.,
496 Cao, J. J., Liu, S. X., Zhang, T., Zhang, R., and Chen, Y. B.: Evolution of aerosol chemistry in
497 Xi'an, inland China, during the dust storm period of 2013-Part 1: Sources, chemical forms and
498 formation mechanisms of nitrate and sulfate, Atmos Chem Phys, 14, 11571-11585, 10.5194/acp-
499 14-11571-2014, 2014.
500 Wang, G. H., Zhang, F., Peng, J. F., Duan, L., Ji, Y. M., Marrero-Ortiz, W., Wang, J. Y., Li, J. J., Wu,
501 C., Cao, C., Wang, Y., Zheng, J., Secrest, J., Li, Y. X., Wang, Y. Y., Li, H., Li, N., and Zhang, R.
502 Y.: Particle acidity and sulfate production during severe haze events in China cannot be reliably
503 inferred by assuming a mixture of inorganic salts, Atmos Chem Phys, 18, 10123-10132,
504 10.5194/acp-18-10123-2018, 2018.
505 Wang, H. C., Wang, H. L., Lu, X., Lu, K. D., Zhang, L., Tham, Y. J., Shi, Z. B., Aikin, K., Fan, S. J.,
506 Brown, S. S., and Zhang, Y. H.: Increased night-time oxidation over China despite widespread
507 decrease across the globe, Nature Geoscience, 16, 217-+, 10.1038/s41561-022-01122-x, 2023.
508 Wang, Y., Hu, M., Wang, Y., Zheng, J., Shang, D., Yang, Y., Liu, Y., Li, X., Tang, R., Zhu, W., Du, Z.,
509 Wu, Y., Guo, S., Wu, Z., Lou, S., Hallquist, M., and Yu, J. Z.: The formation of nitro-aromatic
510 compounds under high NOx and anthropogenic VOC conditions in urban Beijing, China, Atmos.
511 Chem. Phys., 19, 7649-7665, 10.5194/acp-19-7649-2019, 2019.
512 Wang, Z. L., Huang, X., Wang, N., Xu, J. W., and Ding, A. J.: Aerosol-Radiation Interactions of Dust
513 Storm Deteriorate Particle and Ozone Pollution in East China, J Geophys Res-Atmos, 125,
514 10.1029/2020JD033601, 2020.
515 Wu, C., Zhang, S., Wang, G. H., Lv, S. J., Li, D. P., Liu, L., Li, J. J., Liu, S. J., Du, W., Meng, J. J.,
516 Qiao, L. P., Zhou, M., Huang, C., and Wang, H. L.: Efficient Heterogeneous Formation of
517 Ammonium Nitrate on the Saline Mineral Particle Surface in the Atmosphere of East Asia during
518 Dust Storm Periods, Environ Sci Technol, 54, 15622-15630, 10.1021/acs.est.0c04544, 2020.
519 Xiao, Q. Y., Geng, G. N., Xue, T., Liu, S. G., Cai, C. L., He, K. B., and Zhang, Q.: Tracking PM2.5
520 and O3 Pollution and the Related Health Burden in China 2013-2020, Environ Sci Technol, 56,
521 6922-6932, 10.1021/acs.est.1c04548, 2022.
522 Xie, Y. N., Wang, G. H., Wang, X. P., Chen, J. M., Chen, Y. B., Tang, G. Q., Wang, L. L., Ge, S. S.,
523 Xue, G. Y., Wang, Y. S., and Gao, J.: Nitrate-dominated PM2.5 and elevation of particle pH
524 observed in urban Beijing during the winter of 2017, Atmos Chem Phys, 20, 5019-5033,
525 10.5194/acp-20-5019-2020, 2020.
526 Yuan, W., Huang, R. J., Yang, L., Guo, J., Chen, Z., Duan, J., Wang, T., Ni, H., Han, Y., Li, Y., Chen,

https://doi.org/10.5194/egusphere-2025-654
Preprint. Discussion started: 20 March 2025

Q., Chen, Y., Hoffmann, T., and O'Dowd, C.: Characterization of the light-absorbing properties, chromophore composition and sources of brown carbon aerosol in Xi'an, northwestern China, Atmos. Chem. Phys., 20, 5129-5144, 10.5194/acp-20-5129-2020, 2020.

Zhang, F., Wang, Y., Peng, J. F., Chen, L., Sun, Y. L., Duan, L., Ge, X. L., Li, Y. X., Zhao, J. Y., Liu, C., Zhang, X. C., Zhang, G., Pan, Y. P., Wang, Y. S., Zhang, A. L., Ji, Y. M., Wang, G. H., Hu, M., Molina, M. J., and Zhang, R. Y.: An unexpected catalyst dominates formation and radiative forcing of regional haze, P Natl Acad Sci USA, 117, 3960-3966, https://doi.org/10.1073/pnas.1919343117, 2020.

Zhang, R., Wang, G., Guo, S., Zamora, M. L., Ying, Q., Lin, Y., Wang, W., Hu, M., and Wang, Y.: Formation of Urban Fine Particulate Matter, Chemical Reviews, 115, 3803-3855, 10.1021/acs.chemrev.5b00067, 2015.

Zhang, S., Gao, Y. N., Xu, X. B., Chen, L. Y., Wu, C., Li, Z., Li, R. J., Xiao, B. Y., Liu, X. D., Li, R., Zhang, F., and Wang, G. H.: Heterogeneous formation and light absorption of secondary organic aerosols from acetone photochemical reactions: remarkably enhancing effects of seeds and ammonia, Atmos Chem Phys, 24, 14177-14190, 10.5194/acp-24-14177-2024, 2024.

Zhang, X., Liu, J., Parker, E. T., Hayes, P. L., Jimenez, J. L., de Gouw, J. A., Flynn, J. H., Grossberg, N., Lefer, B. L., and Weber, R. J.: On the gas-particle partitioning of soluble organic aerosol in two urban atmospheres with contrasting emissions: 1. Bulk water-soluble organic carbon, Journal of Geophysical Research: Atmospheres, 117, doi.org/10.1029/2012JD017908, 2012.

https://doi.org/10.5194/egusphere-2025-654
Preprint. Discussion started: 20 March 2025

Table 1. Meteorological parameters and concentrations of gaseous and particulate pollutants in $PM_{2.5}$ in Shanghai during the spring 2023 campaign

	Whole campaign	Dust storm	Haze event	Clean period
I Meteorological parameters and gaseous pollutants				
RH (%)	59 ± 14	44 ± 18	61 ± 13	63 ± 9
T (°C)	17 ± 4	17 ± 3	13 ± 3	21 ± 3
$WSOC_g$[a] (μgC m^{-3})	8.0 ± 3.4	6.1 ± 1.5	6.0 ± 1.4	8.2 ± 3.3
Formic $acid_g$[a] (μg m^{-3})	3.2 ± 4.4	1.5 ± 2.6	1.3 ± 1.0	3.4 ± 6.7
Acetic $acid_g$[a] (μg m^{-3})	1.2 ± 2.3	0.9 ± 2.0	0.5 ± 0.4	1.3 ± 2.8
NH_3 (μg m^{-3})	4.9 ± 1.6	5.1 ± 1.6	4.0 ± 0.8	5.3 ± 1.8
II Major components of $PM_{2.5}$				
$PM_{2.5}$ (μg m^{-3})	30 ± 14	39 ± 16	43 ± 16	20 ± 7
PM_{10} (μg m^{-3})	76 ± 89	301 ± 192	58 ± 15	43 ± 19
OC (μgC m^{-3})	5.0 ± 2.7	6.0 ± 5.0	5.7 ± 1.9	3.8 ± 3.2
EC (μgC m^{-3})	1.1 ± 0.6	0.7 ± 0.4	1.1 ± 0.5	0.7 ± 0.5
$WSOC_p$[a] (μgC m^{-3})	3.1 ± 1.3	2.6 ± 0.7	3.0 ± 0.8	2.8 ± 1.7
$WSOC_p$/OC	0.6 ± 0.2	0.5 ± 0.2	0.7 ± 0.1	0.7 ± 0.1
Formic $acid_p$[a] (μg m^{-3})	0.2 ± 0.1	0.1 ± 0.1	0.3 ± 0.1	0.2 ± 0.1
Acetic $acid_p$[a] (μg m^{-3})	0.06 ± 0.04	0.04 ± 0.04	0.1 ± 0.04	0.06 ± 0.04
Oxalic $acid_p$[a] (μg m^{-3})	0.3 ± 0.3	0.2 ± 0.3	0.5 ± 0.4	0.3 ± 0.2
NH_4^+ (μg m^{-3})	3.7 ± 2.5	1.3 ± 1.3	6.8 ± 2.1	2.2 ± 0.9
NO_3^- (μg m^{-3})	7.7 ± 6.5	3.2 ± 2.5	15.2 ± 6.2	2.9 ± 1.5
SO_4^{2-} (μg m^{-3})	4.2 ± 2.6	2.1 ± 2.2	6.8 ± 2.9	3.7 ± 1.8
Ca^{2+} (μg m^{-3})	0.1 ± 0.2	0.6 ± 0.5	0.08 ± 0.05	0.01 ± 0.01
Na^+ (μg m^{-3})	0.2 ± 0.3	0.4 ± 0.1	0.1 ± 0.05	0.2 ± 0.2
Mg^{2+} (μg m^{-3})	0.08 ± 0.06	0.2 ± 0.05	0.04 ± 0.01	0.1 ± 0.02
ALWC[b] (μg m^{-3})	9.6 ± 12.1	2.7 ± 2.2	18.5 ± 14.4	5.3 ± 2.5
pH of $PM_{2.5}$	3.4 ± 0.8	4.8 ± 1.5	3.4 ± 0.3	2.8 ± 0.5
F_p[c]	0.28 ± 0.08	0.3 ± 0.06	0.32 ± 0.06	0.24 ± 0.06

[a]$WSOC_g$, formic $acid_g$ and acetic $acid_g$ are the gas-phase organics while $WSOC_p$, formic $acid_p$, acetic $acid_p$ and oxalic $acid_p$ are the organics in $PM_{2.5}$. [b]ALWC: aerosol liquid water content of $PM_{2.5}$.

[c]$F_p = \frac{WSOC_p}{WSOC_g + WSOC_p}$

https://doi.org/10.5194/egusphere-2025-654
Preprint. Discussion started: 20 March 2025

552 **Table 2**. Concentrations of $WSOC_p$, $WSON_p$, organic acids, and inorganic ions and optical
553 properties of $WSOC_p$ in airborne particles in Shanghai and Tengger Desert region

	Non-dust storm		Dust storm		Tengger Desert
	Fine mode (<2.1μm)	Coarse mode (>2.1μm)	Fine mode (<2.1μm)	Coarse mode (>2.1μm)	PM_{10}
$WSOC_p$ (μgC m^{-3})	2.0	1.8	2.4	3.4	14 ± 7.5
$WSON_p$ (μgN m^{-3})	1.1	0.3	0.7	0.5	ND[c]
PM (μg m^{-3})	19	48	52	367	402 ± 75
Oxalic acid (μg m^{-3})	0.7	0.4	0.3	1.4	0.7
Pyr[a] (μg m^{-3})	0.06	0.09	0.03	0.2	0.03 ± 0.01
MSA[b] (μg m^{-3})	0.1	0.1	0.09	0.5	ND[c]
NACs (ng m^{-3})	0.5	0.9	0.5	1.7	ND[c]
IMs (ng m^{-3})	0.7	0.1	0.5	0.2	ND[c]
Abs_{365} (M m^{-1})	1.9	0.8	2.2	2.6	2.5 ± 0.4
MAC_{365} (m^2 g^{-1})	1.0	0.4	0.9	0.8	0.2 ± 0.09

554 [a] Pyr: pyruvic acid. [b] MSA: methanesulfonic acid. [c]ND: Not Detected

555

https://doi.org/10.5194/egusphere-2025-654
Preprint. Discussion started: 20 March 2025

Figure Caption

Figure 1. Temporal variations in meteorological parameters and concentrations of major components in $PM_{2.5}$ during the spring of 2023 in Shanghai, China.

Figure 2. Factors controlling the gas-to-particle phase partitioning of WSOC in haze (HE) and dust storm (DS) events. (a) F_p as a function of ALWC in HE and DS. (b) ALWC as a function of ammonia partitioning coefficient ($\varepsilon(NH_4^+) = NH_4^+ / (NH_3 + NH_4^+)$) in HE. (c) Dependence of $WSOC_p$ concentrations on ALWC in HE. (d) Linear regression fit for TNH_x versus $WSOC_p$ concentration during HE and DS periods. (e) F_p of WSOCs as a function of pH during HE and DS periods. (f) Linear regression fit for particulate organic acids and metal cations in HE and DS periods.

Figure 3. Size distributions of $WSOC_p$, $WSON_p$, nitro-aromatic compounds (NACs) and imidazoles (IMs) in Shanghai during the non-dust storm (NDS) and dust storm (DS) periods.

Figure 4. Optical properties of $WSOC_p$ of PM_{10} in Tengger Desert regions and TSP in Shanghai during the dust storm (DS) and non-dust storm (DS) periods. (a) Mass absorption coefficient (MAC) of $WSOC_p$. (b) MAC of $WSOC_p$ in the fine (<2.1μm) and coarse (>2.1μm) modes of atmospheric particles in Shanghai.
.

https://doi.org/10.5194/egusphere-2025-654
Preprint. Discussion started: 20 March 2025

578

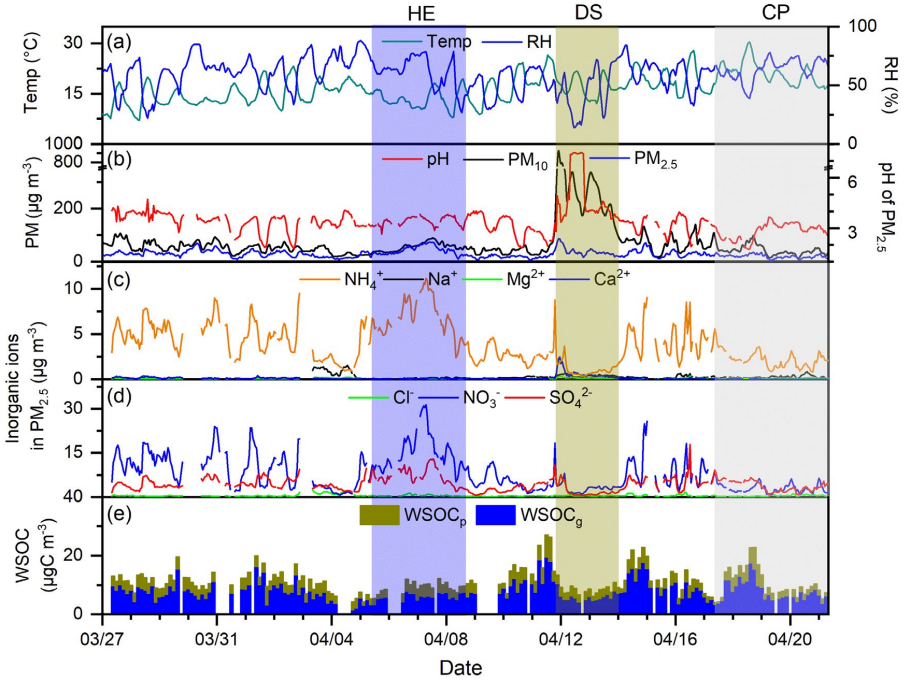

579

580 **Figure 1**. Temporal variations in meteorological parameters and concentrations of major
581 components in $PM_{2.5}$ during the spring of 2023 in Shanghai, China.

582

583

https://doi.org/10.5194/egusphere-2025-654
Preprint. Discussion started: 20 March 2025

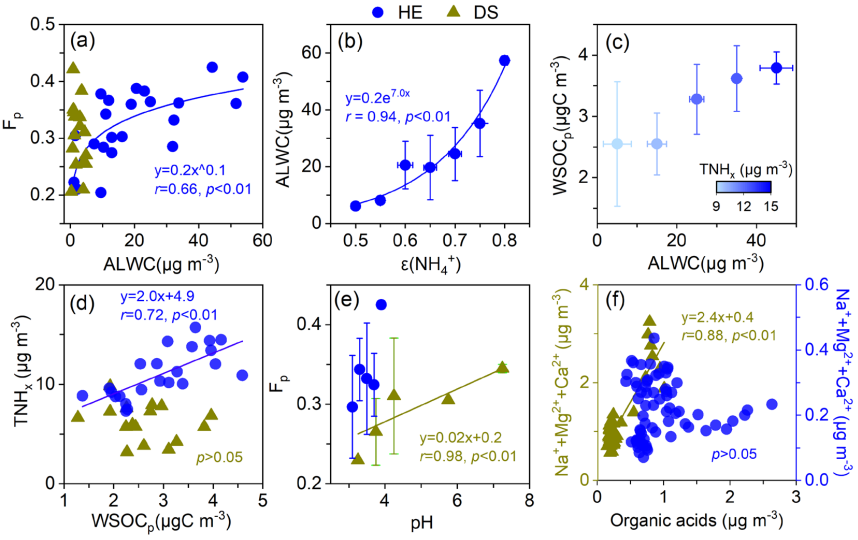

Figure 2. Factors controlling the gas-to-particle phase partitioning of WSOC in haze (HE) and dust storm (DS) events. (a) F_p as a function of ALWC in HE and DS. (b) ALWC as a function of ammonia partitioning coefficient ($\varepsilon(NH_4^+) = NH_4^+ / (NH_3 + NH_4^+)$) in HE. (c) Dependence of $WSOC_p$ concentrations on ALWC in HE. (d) Linear regression fit for TNH_x versus $WSOC_p$ concentration during HE and DS periods. (e) F_p of WSOCs as a function of pH during HE and DS periods. (f) Linear regression fit for particulate organic acids and metal cations in HE and DS periods.

https://doi.org/10.5194/egusphere-2025-654
Preprint. Discussion started: 20 March 2025

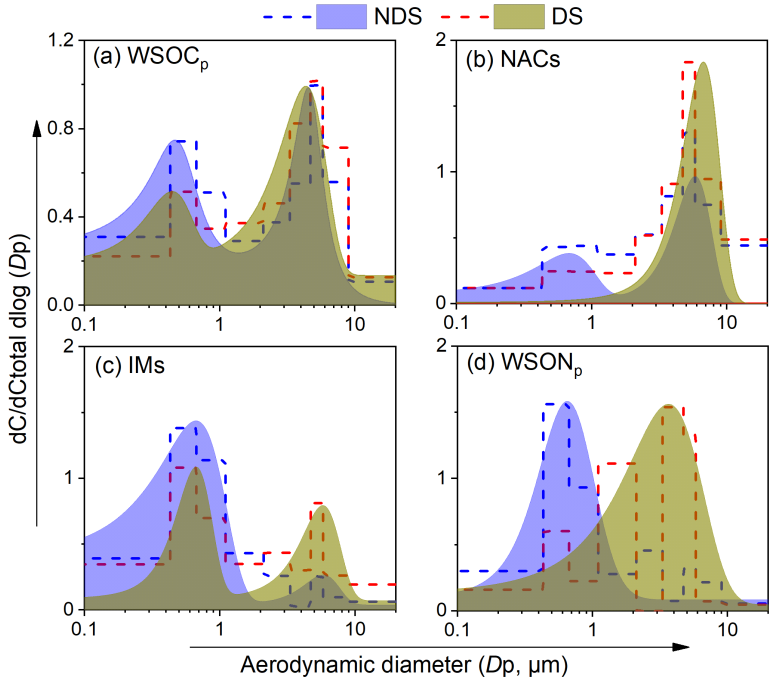

Figure 3. Size distributions of $WSOC_p$, $WSON_p$, nitro-aromatic compounds (NACs) and imidazoles (IMs) in Shanghai during the non-dust storm (NDS) and dust storm (DS) periods.

https://doi.org/10.5194/egusphere-2025-654
Preprint. Discussion started: 20 March 2025

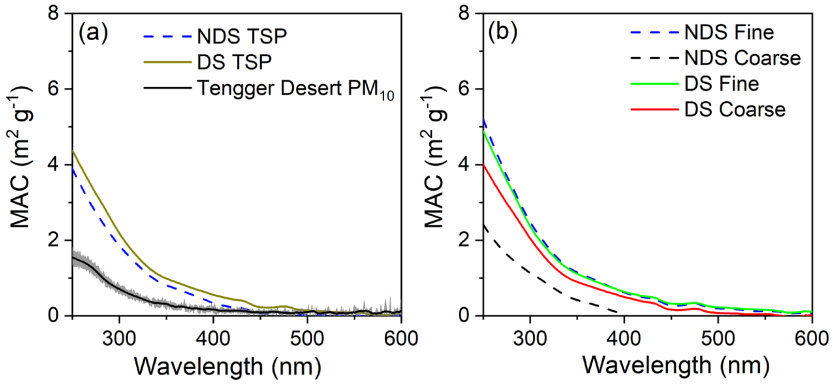

598
599 **Figure 4**. Optical properties of $WSOC_p$ of PM_{10} in Tengger Desert regions and TSP in
600 Shanghai during the dust storm (DS) and non-dust storm (DS) periods. (a) Mass absorption
601 coefficient (MAC) of $WSOC_p$. (b) MAC of $WSOC_p$ in the fine (<2.1μm) and coarse
602 (>2.1μm) modes of atmospheric particles in Shanghai.
603
604
605